Dipole–Dipole Interactions of High-Spin Paramagnetic Centers in Disordered Systems

A. G. Maryasov[1], M. K. Bowman[2], and Yu. D. Tsvetkov[1]

[1] Institute of Chemical Kinetics and Combustion, Russian Academy of Sciences,
Novosibirsk, Russian Federation
[2] Structural Biology and Microimaging, Battelle Northwest, Richland, Washington, USA

Abstract. Dipole–dipole interactions between distant paramagnetic centers (PCs) where at least one PC has spin $S > 1/2$ are examined. The results provide a basis for the application of pulsed electron–electron double resonance method to the measurement of distances between PCs involving high-spin species. A projection operator technique based on spectral decomposition of the secular Hamiltonian is used to calculate electron paramagnetic resonance (EPR) line splitting caused by the dipole coupling. This allows calculation of operators projecting an arbitrary wave function onto high-spin PC eigenstates when the eigenvectors of the Hamiltonian are not known. The effective spin vectors – that is, the expectation values for vector spin operators in the PC eigenstates – are calculated. The dependence of these effective spin vectors on the external magnetic field is calculated. There is a qualitative difference between pairs having at least one integer spin (non-Kramers PC) and pairs of two half-integer (Kramers PC) spins. With the help of these effective spin vectors, the dipolar line shape of EPR lines is calculated. Analytical relations are obtained for PCs with spin $S = 1/2$ and 1. The dependence of Pake patterns on variations of zero-field splitting, Zeeman energy, temperature and dipolar coupling are illustrated.

1 Introduction

The dipole–dipole (d-d) interaction of paramagnetic centers (PCs) depends strongly on their mutual arrangement. This interaction affects the electron paramagnetic resonance (EPR) spectra of the PCs. Thus, e.g., if centers with spin $S = 1/2$ form pairs with the same distance between partners, then the so-called Pake doublet is observed in the EPR spectrum rather than a single absorption line [1] if the Pake doublet is not obscured by broadening caused by other interactions. In the case of a chaotic distribution of PCs in a magnetically dilute system, the d-d interaction leads to the Lorentzian line shape for the EPR absorption [2]. Studying the spectroscopic manifestations of d-d interaction gives unique information about the spatial distribution of PCs initially present in the sample or as modified by different physicochemical processes. Pulsed EPR methods, known

as either PELDOR (pulsed electron double resonance) or DEER (double electron–electron resonance), have been widely used recently for measurement of d-d interactions, because these methods eliminate the masking of relatively weak dipole interactions by inhomogeneous broadening of EPR lines due to other anisotropic interactions. A series of reviews [3–11] describe methods of obtaining information about the spatial distribution of PC by pulsed EPR spectroscopy.

The theory thus far developed to explain PELDOR spectroscopy strictly holds only for $S = 1/2$ spin partners. No systematic discussion of the d-d interaction of high-spin PCs has so far been performed due to the relatively complex problem of describing the high-spin PC state. This description is a necessary step in the study of d-d interactions themselves. The conventional approach has been to generalize equations for $S = 1/2$ to an arbitrary spin assuming that the fine structure or zero-field splitting (ZFS) of the EPR spectrum of the high-spin PC can be neglected compared to the Zeeman interaction (see, e.g., ref. 12) which is not valid in the general case. Most of the studies of paramagnetic clusters with high-spin PCs are devoted to the structure of some particular system, see, e.g., old reviews [13–14] and a few examples from the newest review [11]. These systems have been treated as special cases and the role of ZFS on the d-d interactions has not been studied systematically.

Of special note are the results of ref. 15. The authors give a correct algorithm for calculation of the dipole broadening of EPR lines for a system containing arbitrary spins. However, it has been incorrectly implemented even for PC with isotropic g-tensors because the secular contribution of d-d interactions to the shift of PC energy levels has been calculated not from the total dipole interaction Hamiltonian but only from the A and B type components of the so-called Abragam dipole alphabet [1]. Therefore, the results are suitable only for isotropic PC when the splitting in zero field is negligibly small compared with the Zeeman quantum.

There are data available [16] on the influence of d-d interactions on PCs with $S = 1$. As follows from ref. 16, the d-d interaction can be neglected if the splitting in zero magnetic field gives nondegenerate levels whose splitting exceeds the microwave quantum of the EPR spectrometer. We explain this effect quantitatively below.

Here we systematically consider the manifestation of d-d interactions on doublet spin probes ($S = 1/2$) with PCs whose ground state has $S \geq 1$. This work is motivated by the many biological systems containing high-spin centers which could be studied using intrinsic free radicals or spin probes introduced by site-directed spin labeling techniques. This approach can be applied even when the ZFS value is large compared with the EPR microwave quantum so that it is actually impossible to observe any spectra of the non-Kramers PC. Experimental measurements of doublet–multiplet interactions [17–19] are starting to be reported and require a more complete theoretical description than is currently available.

The first section of this contribution is devoted to the description of a high-spin PC, the effective spin vectors (ESVs) are calculated, these vectors are the

expectation values for vector spin operators in the PC eigenstates. The second part deals with the qualitative difference between Kramers and non-Kramers high-spin PC as the partners in the d-d interaction. The third section formulates the secular part of the Hamiltonian of the d-d interaction for a pair of PCs in terms of their ESVs. Pake multiplets of weakly coupled dipole pairs and their dependence on the system temperature are explained in the fourth section. The final section illustrates the influence of the anisotropic ZFS and of the temperature on the Pake patterns of pairs of PCs one of which is the spin probe with $S = 1/2$, and the other with $S = 1$, in a disordered medium. This paper develops a general method for calculating the broadening from d-d interactions which can be applied to the interpretation of experimentally measured DEER and other types of spectra involving PCs with high spin.

2 Spin Hamiltonian and ESVs for $S \geq 1$

Let us consider a PC having $S \geq 1$. A characteristic feature of such a center is the splitting of its energy levels in the absence of an external magnetic field, the so-called ZFS. This is caused by electrostatic interactions and provides the fine structure in optical spectra of such species. The spin Hamiltonian in this case is of the form

$$\mathscr{H} = \mathscr{H}_Z + \mathscr{H}_{ZFS}. \tag{1}$$

Here, $\mathscr{H}_Z$ is the Zeeman interaction of the PC with the external magnetic field and $\mathscr{H}_{ZFS}$ is the ZFS Hamiltonian.

The Zeeman interaction of paramagnetic particles with the external magnetic field $\mathbf{B}_0 = B_0\mathbf{b}$ (with $\mathbf{b}$ being the unit length vector) may be represented [16] as

$$\mathscr{H}_Z = \beta \mathbf{B}_0^+ \bar{g}\hat{\mathbf{S}}, \tag{2}$$

where β is the Bohr magneton; $\bar{g}$ is the g-tensor of the PC; $\hat{\mathbf{S}}$ is the vector spin operator. The plus symbol superscript denotes the Hermitian conjugate (in this case, it reduces to transposition). All the vectors are taken as columns in the coordinate representation. The properties of the "tensor" $\bar{g}$ are considered in detail by Abragam and Bleaney [16]. Equation (2) can readily be rewritten as

$$\mathscr{H}_Z = \beta B_0 g_{eff} \hat{S}_{z'}, \tag{3}$$

where g_{eff} is the effective value of the g-tensor of the PC $g_{eff} = \sqrt{\mathbf{b}^+ \cdot \bar{g} \cdot \bar{g}^+ \cdot \mathbf{b}}$. The z'-axis is the direction of spin quantization by the Zeeman interaction and is given by the vector $\bar{g}^+\mathbf{b}$,

$$z' \parallel \bar{g}^+\mathbf{b} . \tag{4}$$

Thus, the Zeeman Hamiltonian Eq. (2) (and for the $S = 1/2$ spin probe as well) can be solved (diagonalized) by choosing a suitable quantization axis Eq. (4) for the PC spin.

When the ZFS is nonzero, the Hamiltonian for the high-spin PC cannot be diagonalized by choosing the quantization axis for the spin. The simplest ZFS Hamiltonian is

$$\mathcal{H}_{ZFS} = D\{\hat{S}_Z^2 - S(S+1)/3\} + E\{\hat{S}_X^2 - \hat{S}_Y^2\} \tag{5}$$

in the ZFS coordinate system (X, Y, Z), where D and E are the independent parameters of the ZFS. The ZFS axes are chosen to satisfy the following relation: $0 \le E/|D| \le 1/3$. This can be fulfilled by a simple redefinition of molecular axes (on the problem of the proper choice of the molecular frame see, e.g., ref. 20). Equation (5) gives a complete description of ZFS with $S = 1$ and $3/2$. For PC with higher spin, terms with the fourth ($S = 2$ and $5/2$), sixth ($S = 3$ and $7/2$) and higher even powers of spin operators can appear [16]. In an external magnetic field, the spin Hamiltonian $\mathcal{H}$ equals the sum of the Zeeman Eq. (3) and ZFS Eq. (5) interactions (ignoring the usually much weaker hyperfine interactions),

$$\mathcal{H} = \beta B_0 g_{eff} \hat{S}_{z'} + D\{\hat{S}_Z^2 - S(S+1)/3\} + E\{\hat{S}_X^2 - \hat{S}_Y^2\}. \tag{6}$$

Note that in Eq. (6) the z' and Z axes generally do not coincide; z' is determined by the direction Eq. (4) of the effective magnetic field, and the second one is determined by the ZFS (molecular axes). It is nontrivial to derive general, analytical eigenfunctions and eigenvalues for Hamiltonian Eq. (6) and is possible only for $S = 1$ and $3/2$ (see, e.g., refs. 21–23).

Fortunately, it is possible to describe important properties of the high-spin PC without knowing the exact eigenvalues and eigenstates of the Hamiltonian (6). Let us denote these as ε_m and $|\chi_m\rangle$, respectively, with index $m = -S, -S+1, \ldots, S-1, S$. The numbering is chosen to provide $|\chi_m\rangle = |m\rangle$ when the ZFS vanishes ($D = E = 0$). Here $|m\rangle$ is the eigenfunction of the $\hat{S}_{z'}$ operator with the eigenvalue of m. For further calculations it is useful to use the $2S + 1$ classical vectors $\mathbf{s}_m$ of the effective spin,

$$\mathbf{s}_m = \langle \chi_m | \hat{\mathbf{S}} | \chi_m \rangle. \tag{7}$$

These vectors are the expectation values of the PC spin vector when the system is in its mth eigenstate.

Let us introduce the projection operator $\hat{P}_m = |\chi_m\rangle\langle\chi_m|$, which projects any wave function onto the mth eigenstate. Equation (7) may be rewritten as

$$\mathbf{s}_m = \text{Tr}(\hat{\mathbf{S}}\hat{P}_m), \tag{8}$$

which has the advantage that $\hat{P}_m$ may be calculated (using the theorem for the spectral decomposition of a linear operator) in terms of the Hamiltonian and its

eigenvalues [24] without knowledge of its eigenstates (see also ref. 25 for an example of this approach for HYSCORE spectra calculations and ref. 26 where the Baker–Campbell–Hausdorff problem was solved in closed form),

$$\hat{P}_m = \prod_{j \neq m} \frac{\mathscr{H} - \varepsilon_j}{\varepsilon_m - \varepsilon_j}. \tag{9}$$

Equation (9) is valid if there is no degeneracy in the Hamiltonian Eq. (6) eigensystem. Such is the case when $B_0 \neq 0$, because only accidental degeneracies may occur [20].

Equation (9) clearly shows that the $\hat{P}_m$ is a polynomial of the system Hamiltonian of the order $2S$,

$$\hat{P}_m = C_m \sum_{j=0}^{2S} c_{m,j} \mathscr{H}^j. \tag{10}$$

Here, the coefficients $c_{m,j}$ depend on the eigenvalues ε_n $(-S \leq n \leq +S)$, $c_{m,2S} = 1$, and

$$C_m = \prod_{j \neq m} \frac{1}{\varepsilon_m - \varepsilon_j}. \tag{11}$$

Some of the coefficients $c_{m,j}$ are listed in Table 1.

The projection operators have a very simple form when ZFS vanishes $(D = E = 0)$. In such situation $\mathscr{H} = \mathscr{H}_Z$ and

$$\hat{P}_m = \prod_{j \neq m} \frac{\hat{S}_{z'} - j}{m - j}. $$

Projection operators provide some powerful results without knowledge of exact eigenvalues. For instance, we can calculate the ESV of the mth eigenstate in Eq. (8) with the help of Eq. (10) as

$$\mathbf{s}_m = C_m \sum_{j=1}^{2S} c_{m,j} \mathbf{\sigma}_j. \tag{12}$$

Here, the vectors $\mathbf{\sigma}_j$ $(1 \leq j \leq 2S)$ depend on the form of the Hamiltonian as a whole, $\mathbf{\sigma}_j = \mathrm{Tr}(\hat{\mathbf{S}} \mathscr{H}^j)$, and may be calculated separately in analytical form for different values of S and for different types of ZFS Hamiltonians. For example,

$$\mathbf{\sigma}_1 = \frac{S(S+1)(2S+1)}{3} \hbar \omega_0 \mathbf{k}. $$

Here

$$\hbar \omega_0 = g_{\mathrm{eff}} \beta B_0, \tag{13}$$

Table 1. Coefficients $c_{m,j}$ as functions of the Hamiltonian invariants.

j	$c_{m,j}$
$2S$	1
$2S - 1$	ε_m
$2S - 2$	$\varepsilon_m^2 - \mathrm{Tr}(\mathscr{H}^2)/2$
$2S - 3$	$-\varepsilon_m^3 + \mathrm{Tr}(\mathscr{H}^3)/3 + \varepsilon_m \mathrm{Tr}(\mathscr{H}^2)/2$
$2S - 4$	$\varepsilon_m^4 - \mathrm{Tr}(\mathscr{H}^4)/4 - \varepsilon_m \mathrm{Tr}(\mathscr{H}^3)/3 + \{Tr(\mathscr{H}^2)\}^2/8$
...	...
0	$\prod_{j \neq m} \varepsilon_j = \varepsilon_m^{-1} \det(\mathscr{H})$, if $\varepsilon_m \neq 0$

and the unit vector $\mathbf{k}$ is directed along the z'-axis given in Eq. (4),

$$\mathbf{k} = \bar{g}^+ \mathbf{b} / g_{\mathrm{eff}}. \tag{14}$$

We calculated vectors $\boldsymbol{\sigma}_j$ for spin values 1, 3/2, 2 using Mathematica 5.0. The results for the ZFS Hamiltonian Eq. (5) may be presented in the form

$$\boldsymbol{\sigma}_j = \hbar \omega_0 \bar{T}_j \mathbf{k}, \tag{15}$$

where the three-dimensional (3-D) operators $\bar{T}_j$ are diagonal in the system of the principal axes of the ZFS Hamiltonian. This means that if vector $\mathbf{k}$ is parallel to a principal axis, then all vectors $\boldsymbol{\sigma}_j$ and $\mathbf{s}_m$ are also parallel to the same axis. These operators are not tensors because their components, in some cases, depend on the orientation of the vector $\mathbf{k}$. Such is the case for $j = 4$ with $S = 2$. The "principal" values of operators T are listed in Table 2 for $S = 1$, 3/2, 2. Making use of Eq. (15), one can rewrite Eq. (12) as

$$\mathbf{s}_m = \bar{\Gamma}_m \mathbf{k}, \tag{16}$$

where

$$\bar{\Gamma}_m = \hbar \omega_0 C_m \sum_{j=1}^{2S} c_{m,j} \bar{T}_j. \tag{17}$$

An alternative form of Eq. (16) is

$$\mathbf{s}_m = \frac{\beta}{\hbar \omega_0} \bar{\Gamma}_m \bar{g}^+ \mathbf{B}_0, \tag{18}$$

where Eqs. (13) and (14) were taken into account.

Let us note that when the ZFS vanishes ($D = E = 0$), the ESVs may be calculated directly using their definition in Eq. (7) so that

Table 2. Principal components of operators T for different spin values.

S	j	$T_{j,XX}$	$T_{j,YY}$	$T_{j,ZZ}$
1	1	2	2	2
	2	$-2/3(D - 3E)$	$-2/3(D + 3E)$	$4D/3$
3/2	1	5	5	5
	2	$-4(D - 3E)$	$-4(D + 3E)$	$8D$
	3	$3(3D^2 - 4DE + 13E^2)$ $+ 41/4(\hbar\omega_0)^2$	$3(3D^2 + 4DE + 13E^2)$ $+ 41/4(\hbar\omega_0)^2$	$3(5D^2 + 7E^2)$ $+ 41/4(\hbar\omega_0)^2$
2	1	10	10	10
	2	$-14(D - 3E)$	$-14(D + 3E)$	$28D$
	3	$6(9D^2 - 16DE + 43E^2)$ $+ 34(\hbar\omega_0)^2$	$6(9D^2 + 16DE + 43E^2)$ $+ 34(\hbar\omega_0)^2$	$2(51D^2 + 57E^2)$ $+ 34(\hbar\omega_0)^2$
	4	$-70D^3 + 318D^2E - 642DE^2$ $+ 954E^3 + 31(\hbar\omega_0)^2$ $\times\{-D + 6E + 3D\cos(2\theta^a)$ $+ 6E\cos(2\phi)\sin^2\theta\}$	$-70D^3 - 318D^2E - 642DE^2$ $- 954E^3 + 31(\hbar\omega_0)^2$ $\times\{-D - 6E + 3D\cos(2\theta)$ $+ 6E\cos(2\phi)\sin^2\theta\}$	$248D^3 + 312DE^2$ $+ 31(\hbar\omega_0)^2$ $\times\{5D + 3D\cos(2\theta)$ $+ 6E\cos(2\phi)\sin^2\theta\}$

[a] Here θ and ϕ are polar and azimuthal angles of the external magnetic field direction in the principal system of the PC ZFS tensor.

$$\mathbf{s}_m(D = 0) = m\mathbf{k}. \tag{19}$$

The operator $\vec{\Gamma}_m$ is proportional to the 3-D unity operator $\vec{1}$, $\vec{\Gamma}_m(D = 0) = m\vec{1}$ in this case.

The transition probability between the mth and nth energy levels of the PC may be also calculated to second order in the microwave perturbation with the help of projection operators,

$$w_{m,n} \propto \text{Tr}\{\hat{P}_m\mathbf{b}_1\vec{g}\hat{S}\hat{P}_n\mathbf{b}_1\vec{g}\hat{S}\}, \tag{20}$$

where $\mathbf{b}_1$ is a vector of unit length directed along the magnetic component of the weak, linearly polarized microwave field resonant with the two levels so that $\hbar\omega = |\varepsilon_n - \varepsilon_m|$.

3 Kramers and Non-Kramers PCs in the Case of ZFS Large Compared with Zeeman Interaction

There is no formal difference between integer spin (non-Kramers) and half-integer (Kramers) spin states in the above equations. Yet the ESVs do depend in a different manner on the strength of the external magnetic field B_0 for Kramers and non-Kramers paramagnetic centers because of the presence of degenerate eigenvalues for Kramers centers in zero field.

Let us consider the general case of ZFS Hamiltonian Eq. (5) with D, $E \neq 0$. This Hamiltonian has no degenerate eigenvalues for any integer value of spin. The transition energies are of the order of E in the worst cases [16, 20]. When the external magnetic field is weak compared with the transition energies of the system so that

$$B_0 \ll \frac{E}{g_{\text{eff}}\beta}, \tag{21}$$

the vectors of effective spin are also small,

$$|\mathbf{s}_m| \propto \frac{g_{\text{eff}}\beta B_0}{E} \ll 1. \tag{22}$$

It is possible to say that the magnetic moment (and effective spin) in non-Kramers systems is quenched in weak external magnetic fields and consequently the dipolar broadening vanishes.

The situation is quite different in the case of Kramers systems. In accordance with Kramers theorem, each energy level is at least twofold degenerate in the absence of an external magnetic field. When $D \neq 0$, the degeneracy of Hamiltonian Eq. (5) is exactly twofold. This degeneracy is eliminated in first order by application of an external magnetic field. In the case of the weak magnetic field given in Eq. (21) the only factor in the denominator of Eq. (11) has a value proportional to the Zeeman splitting Eq. (13) thus providing

$$\lim_{B_0 \to 0} |\mathbf{s}_m| = f_m(D, E, \mathbf{b}) \geq \text{const} > 0. \tag{23}$$

This means that Kramers systems always possess magnetic moment (and effective spin).

A non-Kramers system having axial ZFS with $E = 0$ (see Eq. (5)) also has a degenerate eigensystem. In this situation the eigenstates in zero magnetic field are $|\chi(m)\rangle = |m\rangle$ with $\varepsilon_m = D\{m^2 - S(S+1)/3\}$, where the axis Z is taken as the unique quantization axis for the PC spin, and m is the projection of the spin onto this axis. The eigenstate with $m = 0$ is not degenerate, while pairs of eigenstates with the same values of $|m|$ have the same energy. This means that although $|\mathbf{s}_0| \propto g_{\text{eff}}\beta B_0 / |D|$, for $m \neq 0$ an analog of Eq. (23) is valid. We do not consider here the improbable case when the vector $\mathbf{k}$ is perpendicular to the symmetry axis Z of the ZFS Hamiltonian so that the external magnetic field does not eliminate the degeneracy of the eigensystem in first order. Thus, in all external magnetic fields, Kramers PCs will always produce dipolar broadening of other Kramers PCs. Non-Kramers PCs with nondegenerate levels have their dipole spin moments quenched at very low fields and will not produce dipole broadening of other PCs, nor will they be broadened by other PCs.

4 D-D Interaction Hamiltonian for Point Dipoles in the Secular Approximation

In the general case, the d-d interaction for point PCs is described by the Hamiltonian (see, e.g., ref. 16)

$$\mathscr{H}_{dd}^{i,j} = \frac{1}{r_{ij}^3}[(\hat{\boldsymbol{\mu}}_i \cdot \hat{\boldsymbol{\mu}}_j) - 3(\mathbf{n} \cdot \hat{\boldsymbol{\mu}}_i)(\mathbf{n} \cdot \hat{\boldsymbol{\mu}}_j)], \tag{24}$$

where $\mathbf{n}$ is the unit vector in the direction connecting the interacting PCs; r_{ij} is the intrapair distance, and $\hat{\boldsymbol{\mu}}_i$ is the magnetic moment operator of the ith PC, $\hat{\boldsymbol{\mu}}_i = -\beta \vec{\vec{g}}_i \hat{\mathbf{S}}_i$.

The system Hamiltonian for two PCs coupled by d-d interaction is $\mathscr{H} = \mathscr{H}_1 + \mathscr{H}_2 + \mathscr{H}_{dd}^{1,2}$, where $\mathscr{H}_i$ is the spin Hamiltonian of the ith PC given in Eqs. (1) and (6), here $i = 1, 2$. The Hamiltonian Eq. (6) parameters (and spins) may differ for the first and the second PCs and the principal axes of ZFS interactions need not coincide in the general case. We shall use an additional subscript to denote the PC, e.g., $g_{i,\mathrm{eff}}$, S_i, D_i are the effective value of g-tensor, spin, and ZFS parameter of the ith PC, respectively. For spin operators we shall use designations like $\hat{S}_{i,X}$ for principal axes of the ith PC ZFS Hamiltonian.

In this paper we assume (the typical condition in DEER) that the d-d interaction is small and its influence will be taken into account as a first-order perturbation. This suggests the following requirements: the zero-order Hamiltonian $\mathscr{H}_0 = \mathscr{H}_1 + \mathscr{H}_2$ must have the nondegenerate eigenvalues, and all the transition energies should be greater than the dipolar coupling. These requirements may be written in the form

$$\min_{(m_j, n_j) \neq (m_k, n_k)} \left| (\varepsilon_{1,m_j} + \varepsilon_{2,n_j}) - (\varepsilon_{1,m_k} + \varepsilon_{2,n_k}) \right| \gg \left\| \mathscr{H}_{dd}^{1,2} \right\|. \tag{25}$$

Here, m_j, m_k and n_j, n_k number the eigenstates of the 1st and the 2nd PCs, respectively ($m = -S_1, -S_1 + 1, \ldots, S_1$; $n = -S_2, -S_2 + 1, \ldots, S_2$), $\varepsilon_{i,k}$ is kth eigenvalue of ith PC. The total number of eigenstates is $(2S_1 + 1)(2S_2 + 1)$ for the system in question. It is quite natural to number those with a pair of numbers (m,n), where m and n refer to mth and nth eigenstates of the 1st and the 2nd PCs, respectively.

A degeneracy in the zero-order Hamiltonian requires more accurate treatment of the dipole coupling within the degenerate levels. This gives rise to the so-called cross-singular effects in the spectrum [27]. We will not consider such effects here because they can be treated by a simple extension of the approach used below, although resulting in far more complicated expressions.

In the common, simple situation when Eq. (25) is valid, the first-order system eigenstates are products of eigenfunctions of the two PCs Eq. (24) and the projection operator onto the (m,n) system eigenstate is also a product of the individual projection operators,

$$\hat{P}_{(m,n)} = \hat{P}_{1,m}\hat{P}_{2,n}. \tag{26}$$

Here, $\hat{P}_{i,k}$ is the projection operator onto kth eigenstate of ith PC in its own subspace of $(2S_i + 1)$ dimensions. To avoid confusion, we use parentheses for the subscript of projection operators acting in the joint space of the two spins.

To first order in the dipolar perturbation, the energy of the state (m,n) is $\varepsilon_{(m,n)} = \varepsilon_{1,m} + \varepsilon_{2,n} + \Delta_{m,n}$, where the energy correction Δ is $\Delta_{m,n} = \mathrm{Tr}\{\hat{P}_{(m,n)}\mathscr{H}_{dd}^{1,2}\}$. By Eq. (26), one can obtain

$$\Delta_{m,n} = \Delta_0\{(\mathbf{M}_{1,m} \cdot \mathbf{M}_{2,n}) - 3(\mathbf{n} \cdot \mathbf{M}_{1,m})(\mathbf{n} \cdot \mathbf{M}_{2,n})\}, \tag{27}$$

where

$$\Delta_0 = \frac{\beta^2}{r^3}, \tag{28}$$

and the effective dimensionless magnetic moment vector $\mathbf{M}_{i,k}$ of the ith PC in its kth eigenstate is introduced, $\mathbf{M}_{i,k} = \bar{g}_i\mathbf{s}_{i,k}$. Here $\mathbf{s}_{i,k}$ is the ESV of the ith PC in its kth eigenstate, as defined in Eq. (8) and calculated in Eqs. (16) and (18).

5 Pake Multiplets

A high-spin PC has a complicated EPR spectrum due to the influence of the fine interactions. The ZFS gives the possibility of transitions between all possible PC eigenstates under the influence of a resonant microwave field. This means that a PC with spin S may have $S(2S + 1)$ resonance lines in the frequency domain. We write "may have" here because some of the eigenstates may be unpopulated and transitions between two such unpopulated levels will have zero intensity. The number of resonance lines in the magnetic field domain spectrum may be different from that in the frequency domain because the non-monotonic dependence of transition energies on external magnetic field strength can produce so-called looping transitions in the presence of ZFS terms.

We can easily find the selection rules for our system by a generalization of Eq. (20) for the transition probability,

$$w_{(m,n),(j,k)} \propto \mathrm{Tr}\{\hat{P}_{(m,n)}\mathbf{b}_1(\bar{g}_1\hat{\mathbf{S}}_1 + \bar{g}_2\hat{\mathbf{S}}_2)\hat{P}_{(j,k)}\mathbf{b}_1(\bar{g}_1\hat{\mathbf{S}}_1 + \bar{g}_2\hat{\mathbf{S}}_2)\}.$$

For weakly coupled PCs, the factorization Eq. (26) of projection operators is valid so that the spectrum of the system is the sum of two individual spectra,

$$w_{(m,n),(j,k)} = w_{1,m,j}\delta_{n,k} + w_{2,n,k}\delta_{m,j},$$

where $\delta_{i,j}$ is the Kroneker delta $(-S_1 \leq m, j \leq S_1; -S_2 \leq n, k \leq S_2)$. The dipole coupling of the two PCs in question leads to the splitting of each of the EPR lines from both PCs into Pake multiplets, e.g., the transition between the mth

and jth levels of the first PC is split into $2S_2 + 1$ lines having resonance frequencies of $\omega_{1,m\leftrightarrow j}(k)$ in the frequency domain,

$$\hbar\omega_{1,m\leftrightarrow j}(k) = \left| \varepsilon_{1,m} - \varepsilon_{1,j} + \varDelta_{m,k} - \varDelta_{j,k} \right|. \tag{29}$$

Here, k is the index of the second PC eigenstate. Taking into account the weakness of the dipole interaction Eqs. (25) and (27), Eq. (29) may be rewritten as

$$\hbar\omega_{1,m\leftrightarrow j}(k) = \left| \varepsilon_{1,m} - \varepsilon_{1,j} \right| + \delta_{1,m\leftrightarrow j}(k). \tag{30}$$

Here

$$\delta_{1,m\leftrightarrow j}(k) = \varDelta_0 \{ (\delta\mathbf{M}_{1,m\leftrightarrow j} \cdot \mathbf{M}_{2,k}) - 3(\mathbf{n} \cdot \delta\mathbf{M}_{1,m\leftrightarrow j})(\mathbf{n} \cdot \mathbf{M}_{2,k}) \}, \tag{31}$$

$$\delta\mathbf{M}_{1,m\leftrightarrow j} = \text{sign}(\varepsilon_{1,m} - \varepsilon_{1,j})\{\mathbf{M}_{1,m} - \mathbf{M}_{1,j}\}. \tag{32}$$

The relative intensity $I_{1,m\leftrightarrow j}(k)$ of the kth component of the Pake multiplet of the $m \leftrightarrow j$ transition of the first PC is proportional to the population $n_{2,k}$ of the kth level of the second PC given, at equilibrium, by the Boltzmann distribution (see also ref. 12), so that

$$I_{1,m\leftrightarrow j}(k) \propto n_{2,k} = \frac{1}{Z_2}\exp\left(-\frac{\varepsilon_{2,k}}{k_BT}\right), \tag{33}$$

where k_B is the Boltzmann constant, T is the absolute temperature, and Z_2 is the partition function of the second PC,

$$Z_2 = \sum_{k=-S_2}^{S_2} \exp\left(-\frac{\varepsilon_{2,k}}{k_BT}\right). $$

The temperature may strongly affect the dipolar splitting pattern. In the case of low temperatures when

$$|D_2|, E_2 \gg k_BT, \tag{34}$$

only the lowest level(s) will be populated. We shall not consider here all possible cases, but the case of strong ZFS for the second PC will be considered as a brief example for which Eq. (21) is valid. The number of populated levels in this case depends on the type of PC and on the relation between the Zeeman and the mean thermal energies. For a second Kramers PC, the Pake multiplet reduces to a Pake doublet if the Zeeman energy is small so that the populations of the Kramers doublet sublevels are nearly equal, and there will be just a single line if the thermal energy is small so that just the lowest sublevel of the Kramers doublet is populated (see ref. 28 for details). In the case of a non-

Kramers system, the Pake multiplet at very low temperature reduces to a singlet regardless of the relation between thermal and Zeeman energies except in rare curve crossing situations.

6 Examples

The high-spin PC with Hamiltonian Eq. (6) requires 11 parameters for a complete description of the positions of its spectral lines, namely, the ZFS parameters D, and E; three principal values of the g-tensor; three Euler angles relating it to the ZFS frame; and the three components of the external magnetic field $\mathbf{B}_0$. The second PC also requires 11 parameters, eight to describe its Zeeman and ZFS interactions, and three Euler angles relative to the orientations of the two PCs. The point dipole interaction adds three more parameters: the vector $\mathbf{r}$ connecting the two interacting PCs. The temperature T is also required to account for relative intensities of the Pake components.

The total number of parameters N_t in the most general case is 26 in a single crystal. For orientationally random or powder systems, this number is reduced by 2 because of the averaging over possible orientations of the external magnetic field in the molecular frame. In disordered systems, $N_t = 24$, which is too large for a systematic exploration of Pake patterns in the general case. When the anisotropy of the PCs is caused mainly by ZFS interactions so that the g-tensor anisotropies are negligible, the number of parameters may be reduced by 5 for each of PCs, making $N_t = 16$ in a single crystal and $N_t = 14$ in disordered systems. These parameter spaces are still too large to thoroughly explore.

A model situation of an $S = 1/2$, isotropic spin probe interacting with a high-spin, isotropic g-tensor PC is described with 11 parameters for the single crystal and with 9 parameters for a disordered system. These 9 may be reduced to 5 if we scale the Pake pattern of the spin probe in the frequency domain using Eq. (28) and if the ZFS parameters of the second PC are scaled by its Zeeman quantum given in Eq. (13). With five independent variables, it is still quite a challenge to thoroughly explore the full range of patterns that may be encountered. It is an even greater challenge to interpret experimental spectra and obtain a unique set of parameters. In this regard, measurements made at several different temperatures and microwave frequencies, combined with as much a priori information as possible, can be invaluable for obtaining a unique and accurate interpretation of experimental measurements.

Below we discuss two cases where analytical relations for the dipole splitting may be obtained.

$S_1 = S_2 = 1/2$. In the simplest and well-known situation of $S_1 = S_2 = 1/2$ each PC has just two eigenstates and Eq. (19) is valid for both PCs. The d-d interaction produces Pake doublets for both PCs. Equation (30) simplifies to

$$\hbar\omega_1(m) = g_{1,\text{eff}}\beta B_0 + m\Delta_0\{(\bar{g}_1\mathbf{k}_1 \cdot \bar{g}_2\mathbf{k}_2) - 3(\mathbf{n} \cdot \bar{g}_1\mathbf{k}_1)(\mathbf{n} \cdot \bar{g}_2\mathbf{k}_2)\}.$$

Here $m = \pm 1/2$ is the projection of the spin of the second PC onto its quantization axis. Taking into account Eq. (14), the above formula may be written in terms of the external magnetic field direction $\mathbf{b}$,

$$\hbar\omega_1(m) = g_{1,\mathrm{eff}}\beta B_0 + m(\Delta_0 / g_{1,\mathrm{eff}}g_{2,\mathrm{eff}})\{(\bar{G}_1\mathbf{b}\cdot\bar{G}_2\mathbf{b}) - 3(\mathbf{n}\cdot\bar{G}_1\mathbf{b})(\mathbf{n}\cdot\bar{G}_2\mathbf{b})\}.$$

Here tensors G_i ($i = 1$, 2) [16] are used, $\bar{G}_i = \bar{g}_i\bar{g}_i^+$. A detailed analysis of this type of systems is provided in our earlier paper [28], see also refs. 29 and 30. It was shown that centers of the Pake doublet components of an isotropic PC (spin probe or label) do not coincide due to the g-tensor anisotropy of the partner. The line shape of each Pake doublet component is similar to the EPR line shape with nonaxial g- or hyperfine tensors. Moreover, the line shapes of the components change with temperature, while the line shape does not change in the case of isotropic g-tensors. Pairs with an EPR unobservable partner with $g_\perp = 0$ were found to have a "rectangular" or "square-wave" EPR absorption line shape.

Any high-spin PC whose ground state is a Kramers or non-Kramers doublet may behave like a system having effective $S = 1/2$ in the case of large ZFS Eq. (21) if the low temperature condition Eq. (34) holds. The anisotropy of the g-tensor for this effective spin may be very large and will depend mostly on the E/D ratio and on total S [31]. Equation (18) may be used with the g-tensor for the effective spin, but only the two states having the lowest energies should be considered. Also, when the second PC is a Kramers system with ZFS large compared with the Zeeman interaction but does not meet the low-temperature condition Eq. (34), each pair of levels that are degenerate at zero field can be treated as a separate spin with effective $S = 1/2$ and its own g-tensor. The resonance line of the first PC will be approximated well by the superposition of Pake doublets from each pair of effective $S = 1/2$ levels scaled by the appropriate Boltzmann factors.

$S_1 = 1/2$, $S_2 = 1$. A doublet–triplet pair shows the effects of weak dipole coupling. The single resonance line of the first PC having $S = 1/2$ is split into a triplet (usually overlapping), while each of three resonance lines of the 2nd triplet PC with $S = 1$ is split into Pake doublets.

It is easy to calculate matrix elements of the operators $\bar{\Gamma}_{2,m}$ for the triplet PC because there are only two terms in Eq. (17),

$$\bar{\Gamma}_{2,m} = \alpha_{2,m}[\varepsilon_{2,m}\bar{1} + \bar{D}_2]. \tag{35}$$

Here $\alpha_{2,m} = 2g_{2,\mathrm{eff}}\beta B_0 C_{2,m}$ and $\bar{D}_2$ is the 3-D ZFS tensor. The ZFS Hamiltonian Eq. (5) of the triplet PC may be written as $\mathscr{H}_{2,\mathrm{ZFS}} = \hat{S}_2\bar{D}_2\hat{S}_2$ with principal values of $E - D/3$, $-E - D/3$, $2D/3$. Let us emphasize that the elements of Γ depend on the direction of the external magnetic field because the eigenvalues $\varepsilon_{2,m}$ and $g_{2,\mathrm{eff}}$ (if the g-tensor of the triplet PC is anisotropic) depend on this direction. Figure 1 illustrates the dependence of the ESVs $s_{2,m}$ given in Eq. (16) and of the square of their length on the orientation of the external magnetic field and its strength, and on the parameters of ZFS. This graphic was calculated for
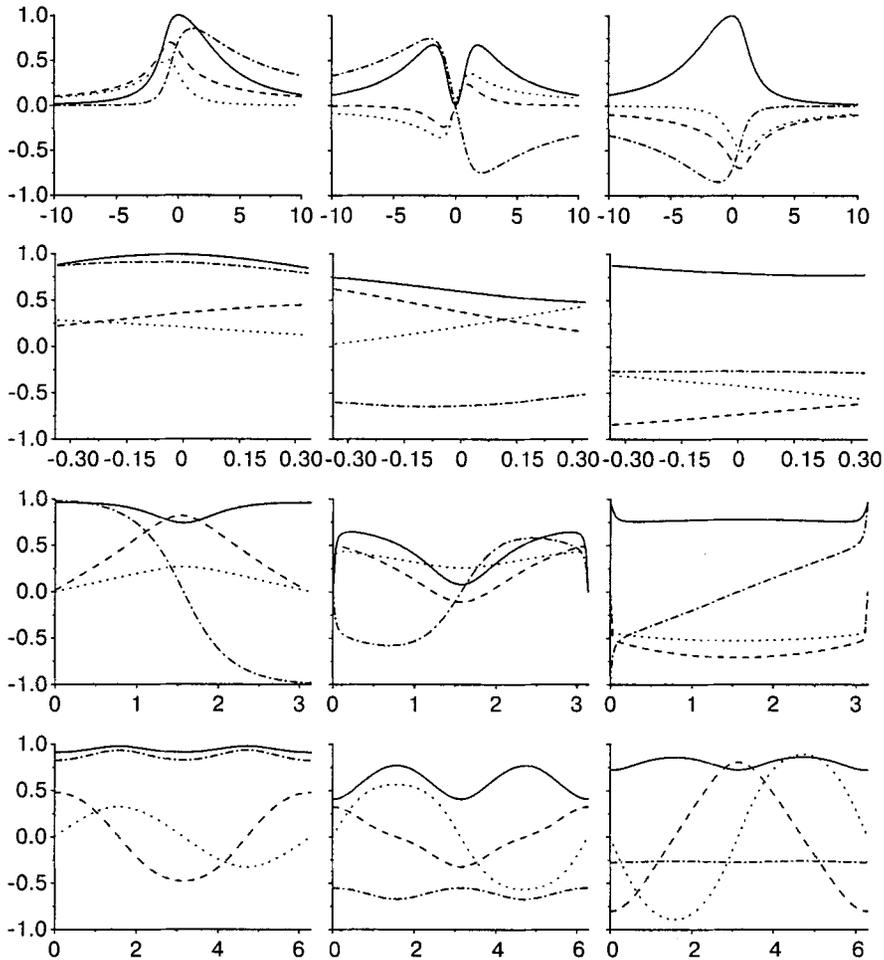
Fig. 1. Dependence of the ESVs on the spin Hamiltonian parameters for a triplet PC with isotropic g-tensor. The basic set of parameters was as follows: $D/g\beta B_0 = 1$, $E/D = 0.2$, $\theta = \pi/4$, $\phi = \pi/6$, where θ and ϕ define the orientation of the external magnetic field in the ZFS frame. Each column corresponds to the number of the PC eigenstate m: left, $m = 1$; middle, $m = 0$; right, $m = -1$. Each row illustrates the dependence of the vectors on varied parameter: top, $D/g\beta B_0$; second, E/D; third, polar angle θ (rads); bottom, azimuthal angle ϕ (rads), while the rest of the parameters are held constant. The solid line shows the square of length of the respective effective vector, $|s_m|^2$, its components in the ZFS frame are shown as dashed (X), dotted (Y), and dashed-dotted (Z) lines. The ESVs decrease drastically as the absolute value of $D/g\beta B_0$ increases, see the top row. The smoothest dependence occurs for the E/D value. The dependence on angles, especially on azimuthal one, clearly demonstrates the nonlinearity of Eq. (18).

a triplet PC with isotropic g-tensor. Figure 2 illustrates the asymptotic quenching of the effective spin moment in accordance with Eq. (22).

For spin $S_2 = 1$ the eigenvalues of the Hamiltonian Eq. (6) may be presented in final form [21–22, 25], so that
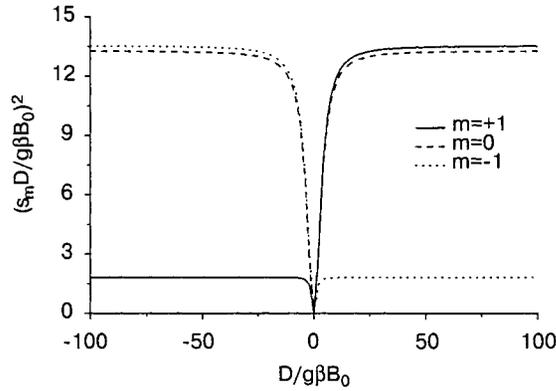
Fig. 2. Asymptotic dependence of the ESVs of triplet PC in the limit of low external magnetic field. Parameters are the same as for the top row in Fig. 1 but the range of D variation is 10 times greater. Eigenstate numbers are indicated for the three lines. The graph shows that Eq. (22) is nearly exact when $E/g\beta B_0 > 5$, E/D was taken as 0.2 for this example.

$$\varepsilon_{2,m} = \left(\frac{4p_2}{3}\right)^{1/2} \cos\left[\frac{\lambda_2 + 2\pi(m+2)}{3}\right]. \tag{36}$$

Here $m = -1, 0, 1$ and

$$p_2 = \frac{1}{2}\mathrm{Tr}(\mathscr{H}_2^2) = \beta^2 \mathbf{B}_0^+ \cdot \bar{G}_2 \cdot \mathbf{B}_0 + \frac{1}{2}\mathrm{Tr}\{\bar{D}_2^2\}, \tag{37}$$

parameter λ is defined by the relation

$$\cos\lambda_2 = \frac{q_2}{2}\left(\frac{3}{p_2}\right)^{3/2},$$

$$q_2 = \frac{1}{3}\mathrm{Tr}(\mathscr{H}_2^3) = \beta^2 \mathbf{B}_0^+ \cdot \bar{g}_2 \cdot \bar{D}_2 \cdot \bar{g}_2^+ \cdot \mathbf{B}_0 - \frac{1}{3}\mathrm{Tr}\{\bar{D}_2^3\}.$$

With respect to the classical definition [21, 22], the sign of p_2 in Eq. (37) is changed for simplicity and the invariants rather than the coordinate forms are used for parameters.

The eigenvalues Eq. (36) possess an important symmetry,

$$\varepsilon_{2,m}(-\bar{D}) = -\varepsilon_{2,-m}(\bar{D}), \tag{38}$$

because $\cos\lambda_2$ changes its sign when parameters D and E change sign simultaneously thus providing $\lambda_2(-\bar{D}) = \pi - \lambda_2(\bar{D})$. This relation leads to Eq. (38) after simple algebra. The consequence is another important symmetry,

$$\vec{\Gamma}_{2,\mathrm{m}}(-\vec{D}_2) = -\vec{\Gamma}_{2,-\mathrm{m}}(\vec{D}_2).$$

Let us calculate the Pake multiplets for each paramagnetic center. The single line of the first PC is split into a triplet because of its d-d interaction with the second PC. The positions of the triplet lines are given in Eqs. (30)–(32), in our case

$$\hbar\omega_1(m) = g_{1,\mathrm{eff}}\beta B_0 + \frac{\Delta_0}{g_{1,\mathrm{eff}}g_{2,\mathrm{eff}}}\{(\vec{G}_1\mathbf{b}\cdot\vec{g}_2\vec{\Gamma}_{2,m}\vec{g}_2^+\mathbf{b})$$

$$- 3(\vec{n}\cdot\vec{G}_1\mathbf{b})(\vec{n}\cdot\vec{g}_2\vec{\Gamma}_{2,m}\vec{g}_2^+\mathbf{b})\}. \tag{39}$$

Here $m = -1, 0, 1$. Each of the three transitions of the second PC is split into a doublet, so that

$$\hbar\omega_{2,j\leftrightarrow n}(m) = \hbar\left|\Omega_2^{j,n}\right| + m\frac{\Delta_0}{g_{1,\mathrm{eff}}g_{2,\mathrm{eff}}}\{(\vec{G}_1\mathbf{b}\cdot\vec{g}_2\delta\vec{\Gamma}_{2,j\leftrightarrow n}\vec{g}_2^+\mathbf{b})$$

$$- 3(\mathbf{n}\cdot\vec{G}_1\mathbf{b})(\mathbf{n}\cdot\vec{g}_2\delta\vec{\Gamma}_{2,j\leftrightarrow n}\vec{g}_2^+\mathbf{b})\}, \tag{40}$$

where $m = \pm 1/2$, $\Omega_2^{j,n}$ is the undisturbed transition frequency of the triplet PC [22],

$$\hbar\Omega_2^{j,n} = \varepsilon_{2,j} - \varepsilon_{2,n} = 2\sqrt{p_2}\,\mathrm{sign}[n - j]\xi_{2,j+n+4}, \tag{41}$$

$$\xi_{2,n} = \sin\left[\frac{\lambda_2 + \pi n}{3}\right],$$

and

$$\delta\vec{\Gamma}_{2,j\leftrightarrow n} = \mathrm{sign}(\varepsilon_{2,j} - \varepsilon_{2,n})(\vec{\Gamma}_{2,j} - \vec{\Gamma}_{2,n})$$

$$= 2g_{2,\mathrm{eff}}\beta B_0\mathrm{sign}(\varepsilon_{2,j} - \varepsilon_{2,n})\{\vec{1}(C_{2,j}\varepsilon_{2,j} - C_{2,n}\varepsilon_{2,n}) + \vec{D}_2(C_{2,j} - C_{2,n})\}. \tag{42}$$

The upper line in Eq. (42) is rather general for all values of S_2, the lower line is based on Eq. (35) and is valid for $S_2 = 1$ only. In the case of weak anisotropy in the tensor $\vec{g}_2$, the value of p_2 is independent of orientation and the transition frequencies Eq. (41) are presented in refs. 21–22 and 25.

Although Eqs. (39) and (40) are valid for interacting PCs with $S_1 = 1/2$ and arbitrary S_2, analytical expressions for $\vec{\Gamma}_2$ are available now only for the case of $S_2 = 1/2$ and 1, see Eq. (35).

When the g-tensor anisotropy of both PCs is negligible, it is useful to re-write Eq. (39) in the dimensionless presentation described above,

$$\tilde{\omega}(m,\mathbf{b}) = \frac{\hbar\omega_1(m) - g_1\beta B_0}{g_1g_2\Delta_0} = \{(\mathbf{b}\cdot\vec{\Gamma}_{2,m}\mathbf{b}) - 3(\mathbf{n}\cdot\mathbf{b})(\mathbf{n}\cdot\vec{\Gamma}_{2,m}\mathbf{b})\}.$$
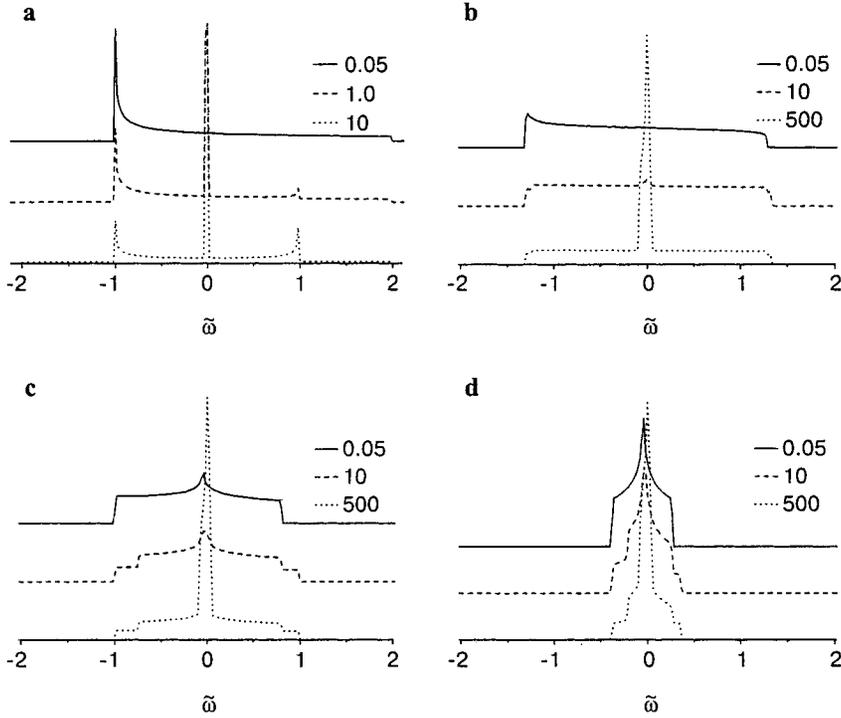
Fig. 3. Dependence of the Pake pattern on ZFS and temperature of isotropic spin label $(S = 1/2)$ caused by dipole coupling with a triplet $(S = 1)$ PC. Temperatures are indicated in units of Zeeman quantum of the triplet PC for the three lines in each panel. **a** Isotropic triplet PC which produces a standard Pake pattern with three components whose amplitudes are temperature dependent. **b** ZFS makes the non-Kramers doublet be the ground state of the triplet PC. $D = -40$, $E = 0$, $\theta = \pi/3$. **c** ZFS removes all degeneracy of the triplet PC, $D = -40$, $E = 0.4$, $\theta = \pi/3$, $\phi = \pi/6$. The relatively small E term leaves the triplet PC with considerable effective spin to broaden the doublet PC. **d** Parameters are the same as for **c** but $E = 2$. Here the effective spin of the triplet is significantly quenched, reducing the dipolar broadening in the Pake pattern.

Here g_i is the g-factor of the ith PC. Making use of Eq. (35), for the triplet PC, one can obtain

$$\tilde{\omega}(m,\mathbf{b}) = \alpha_{2,m}\{\varepsilon_{2,m}[1 - 3(\mathbf{n} \cdot \mathbf{b})^2] + (\mathbf{b} \cdot \bar{D}_2\mathbf{b}) - 3(\mathbf{n} \cdot \mathbf{b})(\mathbf{n} \cdot \bar{D}_2\mathbf{b})\}.$$

In the absence of ZFS, the right-hand side of this equation is equal to the well-known $m(1 - 3\cos^2\theta)$ with θ being the angle between vectors $\mathbf{r}$ and $\mathbf{B}_0$.

The Pake pattern of the first PC with $S = 1/2$ in a disordered system may be written in dimensionless units as

$$U(\tilde{\omega}) = \sum_m \int_{-1}^{1} \mathrm{d}(\cos\theta) \int_0^{2\pi} \mathrm{d}\phi \frac{\delta(\tilde{\omega} - \tilde{\omega}(m,\mathbf{b}))}{Z_2(\mathbf{b})} \exp\left(-\frac{\varepsilon_{2,m}(\mathbf{b})}{k_BT}\right).$$
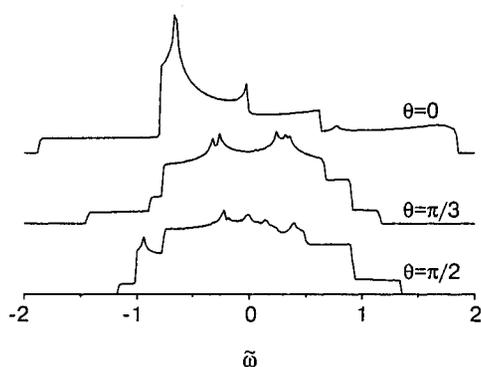
Fig. 4. Pake patterns of isotropic spin label ($S = 1/2$) caused by dipole coupling with a triplet ($S = 1$) PC with $D = 2$, $E = 0.4$, $\phi = \pi/6$ in the high-temperature approximation. The angles θ and ϕ define the orientation of the vector $\bar{n}$ in the ZFS frame. The energy is in units of the Zeeman quantum of triplet PC.

Here θ and ϕ are polar and azimuthal angles of the magnetic field direction in the molecular frame of the high-spin PC, $\delta(x)$ is the Dirac delta-function. The Boltzmann population Eq. (33) is taken into account. Appearance of the delta-function under the integral sign allows, in principle, simplification of the equation, but this requires solving the equation $\tilde{\omega} - \tilde{\omega}(m, \mathbf{b}) = 0$ with respect to the direction of the vector $\mathbf{b}$. This is not a simple task because components of the operator Γ given in Eq. (35) also depend on the direction of the external magnetic field.

For PCs with isotropic g-tensors, Fig. 3 illustrates the dependence of the frequency domain Pake patterns on ZFS parameters of the second PC and on the temperature. The changes within each panel are caused by changes in the Boltzmann population among the triplet PC as the temperature changes. The changes between panels are due to quenching of the spin or dipole moment of the triplet as the degeneracies at low field of this non-Kramers PC are removed.

Figure 4 shows that the pair geometry has strong impact on the Pake pattern as the orientation of the triplet ZFS axes relative to the direction between the two PCs is changed.

7 Conclusions

The d-d interactions of high-spin paramagnetic centers in the secular approximation for point dipoles may be described using vectors of the effective spins for each PC. These vectors are the expectation values of the spin vector operator when the PC is in one of its eigenstates, so the whole set consists of $2S + 1$ vectors for a PC having spin S. To calculate these vectors we use spectral decomposition of the PC Hamiltonian based on the Caley–Hamilton theorem. This technique allows calculation of projection operators onto the PC eigenstates using the Hamiltonian eigenvalues without calculation of its eigenvectors. We find

that these ESVs for spins up to 2 are related to the external magnetic field via the formally linear equation (18). Linearity occurs only in the absence of ZFS, which is always the case for spin $S = 1/2$. For higher spins, matrix elements of the operator Γ also depend on the external magnetic field making this relation nonlinear in the presence of ZFS. Analytical expressions are derived for spin $S = 1$ in the weak d-d interaction limit.

The ESVs behave qualitatively differently for Kramers (half-integer spin) and non-Kramers (integer spin) PCs in the limit that the external magnetic field is weak compared with the ZFS. For non-Kramers systems these vectors are proportional to the ratio of Zeeman energy to the ZFS, reaching zero at low fields. The splittings of the EPR spectra caused by dipole interactions with such non-Kramers PCs vanish at low fields. For Kramers PCs, in contrast, the ESVs tend to limiting nonzero values when external magnetic field decreases and the Pake patterns are always produced.

The d-d interaction leads to the appearance of Pake patterns in EPR spectra. Variations of these patterns with temperature and external magnetic field strength (microwave quantum of EPR spectrometer) can provide important information for the structure determination of a dipole-coupled pair of PCs if the number of parameters to be determined can be suitably constrained. To this end, it is desirable to perform DEER measurements of long-range distances involving high-spin PCs over a wide range of microwave frequencies, magnetic fields, temperatures, and frequency offsets.

Acknowledgments

References

1. Abragam A.: Principles of Nuclear Magnetism. Oxford: Clarendon 1961.
2. Anderson P.W.: Comp. Rend. **82**, 342 (1951)
3. Salikhov K.M., Semenov A.G., Tsvetkov Yu.D.: Elektronnoe Spinovoe Ekho i Ego Primenenie, chapt. 3. Novosibirsk: Nauka 1976.
4. Salikhov K.M., Tsvetkov Yu.D. in: Time Domain Electron Spin Resonance (Kevan L., Schwartz R.N., eds.), p. 231. New York: Wiley 1979.
5. Raitsimring A.M., Salikhov K.M.: Bull. Magn. Reson. **7**, 184 (1985)
6. Dzuba S.A., Kawamori A.: Concepts Magn. Reson. **8**, 49 (1996)
7. Milov A.D., Maryasov A.G., Tsvetkov Yu.D.: Appl. Magn. Reson. **15**, 107 (1998)

8. Eaton G.R., Eaton S.S., Berliner L.J. (eds.): Distance Measurements in Biological Systems by EPR. Biological Magnetic Resonance, vol. 19. New York: Kluwer Academic/Plenum 2000.
9. Freed J.H.: Annu. Rev. Phys. Chem. **51**, 655 (2000)
10. Prisner T., Rohrer M., MacMillan F.: Annu. Rev. Phys. Chem. **52**, 279 (2001)
11. Dzuba S.A.: Usp. Khim. **74**, 686 (2005)
12. Altshuler S.A., Mokeev A.A.: Fiz. Tverd. Tela (Leningrad) **11**, 35 (1969)
13. Smith T.D., Pilbrow J.R.: Coord. Chem. Rev. **13**, 173 (1974)
14. Yablokov Yu.V., Voronkova V.K., Mosina L.V.: Paramagnitnyi Rezonans Obmennykh Klasterov. Moscow: Nauka 1988.
15. Grant W.J.C., Strandberg M.W.P.: Phys. Rev. **135**, A715 (1964)
16. Abragam A., Bleaney B.: Electron Paramagnetic Resonance of Transition Ions. London: Oxford University Press 1970.
17. Koulougliotis D., Tang X.-S., Diner B.A., Brudwig G.W.: Biochemistry **34**, 2850 (1995)
18. Hara H., Kawamori A.: Appl. Magn. Reson. **13**, 241 (1997)
19. White G.F., Ottignon L., Field S., Marritt S., Cheesman M.R., Oganesyan V.S., Thompson A.J., Yap L.-L., Gennis R.B. in: Advanced Techniques and Applications of EPR. Abstracts of 39th Annual International Meeting of Electron Spin Resonance Group of Royal Society of Chemistry, Edinburgh, UK, 2006, P.66.
20. Gaffney B.J., Silverstone H.J. in: EMR of Paramagnetic Molecules. Biological Magnetic Resonance, vol. 13 (Berliner L.J., Reuben J., eds.), p. 1. New York: Plenum 1993.
21. Muha G.M.: J. Chem. Phys. **73**, 4139 (1980)
22. Muha G.M.: J. Magn. Reson. **49**, 431 (1982)
23. Muha G.M.: J. Magn. Reson. **53**, 85 (1983)
24. Broida J.G., Williamson S.G.: Comprehensive Introduction to Linear Algebra. Reading, Mass.: Addison-Wesley 1989.
25. Maryasov A.G., Bowman M.K.: J. Phys. Chem. B **108**, 9412 (2004)
26. Untidt T.S., Nielsen N.C.: Phys. Rev. E **65**, 021108 (2002)
27. Zeer E.P., Zobov V.E., Falaleev O.V.: Novye Effekty v YaMR Polikristallov. Novosibirsk: Nauka 1991.
28. Bedilo A.F., Maryasov A.G.: J. Magn. Reson. A **116**, 87 (1995)
29. Maryasov A.G., Dzuba S.A., Salikhov K.M.: J. Magn. Reson. **50**, 432 (1982)
30. Kurshev V.V., Raitsimring A.M., Salikhov K.M.: Fiz. Tverd. Tela (Leningrad) **30**, 420 (1988)
31. Hagen W.R.: Adv. Inorg. Chem. **38**, 165 (1992)

Authors' address: Alexander G. Maryasov, Institute of Chemical Kinetics and Combustion, Russian Academy of Sciences, Institutskaya ulitsa 3, Novosibirsk 630090, Russian Federation
E-mail: maryasov@kinetics.nsc.ru